Journal of Chemical Health Risks

www.jchr.org

JCHR (2025) 15(6), 1189-1196 | ISSN:2251-6727

Synthesis, Spectral Characterization and Biological Studies of a Novel Silver Complex of N-[2-Hydroxy-3-Methylbenzyl] valine Ligand

Mohd Shahzad[1,*], Naman Chaudhary[1], Shasti Ballabh Mishra[2]

[1]Department of Chemistry, M.B.G. P.G College, Haldwani (Nainital)-263139, India

(Received: 27 September 2025 Revised: 05 October 2025 Accepted: 18 November 2025)

KEYWORDS

N-[2-Hydroxy-3-methyl benzyl]valine
Transition metal complex
Spectral characterization
DFT calculation
Biological activities

ABSTRACT:
A novel silver(I) complex of N-[2-hydroxy-3-methylbenzyl]valine [N-(2-HMBV-3)] was synthesized and extensively characterized through FTIR, UV-Vis, NMR spectroscopy, density functional theory (DFT) calculations and SEM morphology. FTIR spectra revealed clear shifts in the ν(C=O) and O–H/N–H stretching regions, along with new Ag–O and Ag–N bands, confirming metal–ligand coordination. UV–Vis analysis indicated pronounced bathochromic shifts in $\pi \rightarrow \pi^*$ and CT/MLCT transitions, consistent with ligand-to-metal charge transfer (LMCT) and stabilization of the chelated framework. Biological evaluations demonstrated that the silver complex (AgL) exhibited significantly higher activity than the parent ligand (L). Antimicrobial assays revealed superior inhibition against *Escherichia coli* and *Aspergillus niger*, while antioxidant studies showed improved radical scavenging efficiency in the DPPH assay. Cytotoxicity screening on MCF-7 breast cancer cells highlighted stronger dose-dependent inhibition, with AgL displaying enhanced ROS-mediated anticancer potential.

1. Introduction

Transition metal complexes have attracted significant attention in medicinal chemistry due to their diverse coordination environments, tunable redox properties and potential to interact selectively with biological targets [1]. Among them, complexes derived from amino acid based ligands have shown demonstrated prominent antioxidant, antimicrobial and anticancer properties owing to their ability to chelate metals through oxygen and nitrogen donor atoms, thereby modulating the physico-chemical and biological behaviour of the resulting complexes [2].

In recent years, amino acids based ligands have emerged as versatile scaffolds in coordination chemistry, combining the biological compatibility of amino acids with the enhanced binding ability of aromatic or phenolic moieties [3]. Such ligands exhibit amphiphilic properties, improve water solubility and can mimic biomolecular recognition processes [4]. Several studies have shown that amino acid–metal complexes can inhibit microbial growth and induce cytotoxicity in cancer cells through mechanisms such as DNA binding, reactive oxygen species (ROS) generation and enzyme inhibition [5].

Earlier research on cresol and benzyl derivatives complexed with transition metals like Pd(II), Cu(II) and Ni(II) reported significant bioactivity, particularly against Gram-positive bacteria and negative bacteria [6]. These ligands benefit from the electron-donating hydroxyl group, which enhances metal–ligand stability and bioavailability. Similarly, valine- and glycine-based complexes have been found to disrupt bacterial cell wall synthesis and inhibit tumor cell proliferation, indicating the potential of amino acid frameworks for therapeutic applications [7]. Silver complexes derived from amino acid based ligands as potent antimicrobial and anticancer agents due to their unique mechanism of action binding [8].

The present study aims to synthesize and characterize Silver(I) complexes of N-[*o*-hydroxy methyl substituted benzyl]valine, evaluating their anticancer, antioxidant and antimicrobial activities. The complex will be thoroughly characterized using FTIR, UV-Vis, ^{1}H NMR, ^{13}C NMR, density functional theory (DFT), SEM analysis to understand structural, electronic and binding characteristics. this research seeks to uncover new biological potentials of silver–amino acid–phenolic frameworks, potentially leading to therapeutic candidates with anticancer properties, antioxidant and antimicrobial properties.

2. Experimental

Analytical grade reagents and solvents were used directly without further purification. Structural characterization was carried out by FT-IR (4000-400 cm^{-1}) and ^{1}H NMR

Journal of Chemical Health Risks
www.jchr.org
JCHR (2025) 15(6), 1189-1196 | ISSN:2251-6727

spectroscopy (Bruker 400 MHz, DMSO-d_6), confirming metal–ligand interactions. The antimicrobial activity of novel ligand N-[2-hydroxy-3-methylbenzyl]valine [N-(2-HMBV-3)] and its Ag(I) complex was tested against *E. coli* and *A. niger* using standard drugs and MIC values were determined. Antioxidant potential was evaluated *via* DPPH radical scavenging assay, while cytotoxicity was assessed by MTT assay on MCF-7 breast cancer cells. The IC_{50} values were calculated using GraphPad Prism, with data presented as Mean ± SEM.

2.1 Synthesis of N-[2-hydroxy-3-methylbenzyl]valine [N-(2-HMBV-3)] (L): For the synthesis of ligand N-[2-hydroxy-3-methyl-benzyl]valine, 0.01 mol each of *o*-cresol (1.08 g), valine (1.17 g) and sodium acetate (1.36 g) were dissolved in 50 mL of formalin and glacial acetic acid to form a uniform solution. A 40% formalin solution was then added dropwise while maintaining the reaction mixture at 60-80 ºC on a water bath for 2-3 h. The mixture was further kept in a water bath for 12-14 h with occasional stirring and after cooling, a viscous yellowish mass was obtained. The crude ligand was treated with distilled water, filtered and recrystallized using NaOH and 50% HCl. The resulting solid was oven-dried at 20-30 ºC for 2-3 days to yield the purified ligand (**Scheme-I**).

2.2 Synthesis of metal complex (AgL): The 1:1 metal complex was synthesized by reacting 0.01 mol of ligand [2-hydroxy-3-methylbenzyl]valine ([N-(2-HMBV-3)], 2.37 g) with 0.01 mol of silver acetate (1.66 g). Each component was first dissolved separately in 20 mL of DMSO and 20 mL of distilled water to obtain clear solutions, which were then combined. The reaction mixture was heated on a water bath at 60-80 ºC for 12-14 h to facilitate complex formation. After completion, the resulting precipitate was filtered, washed with distilled water and dried at room temperature (20-30 ºC), yielding the anhydrous silver complex of 2-HMBV-3 (**Scheme-II**).

3. Result and discussion

3.1 FTIR spectra: The FTIR spectrum of the free ligand displays characteristic absorptions corresponding to its

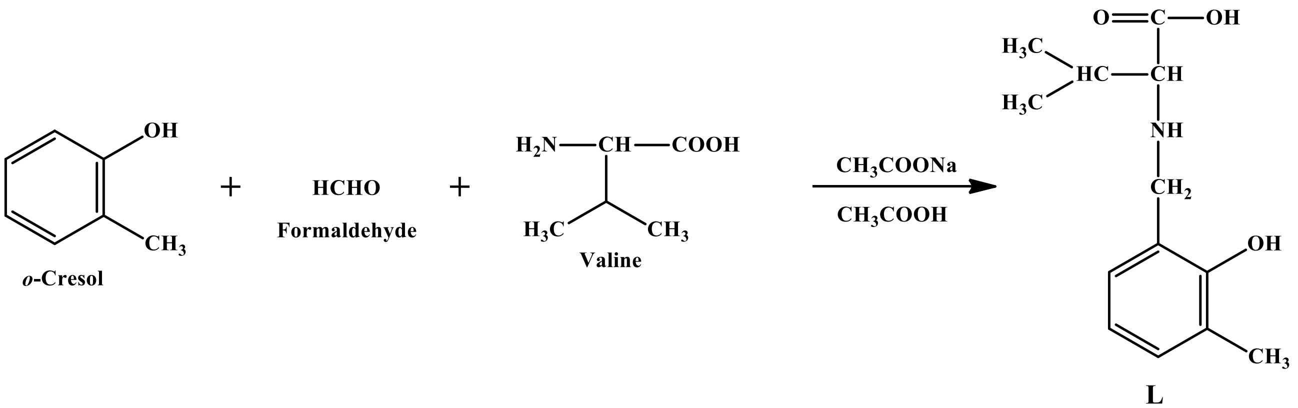

Scheme-I: Synthesis of ligand N-2-HMBV-3

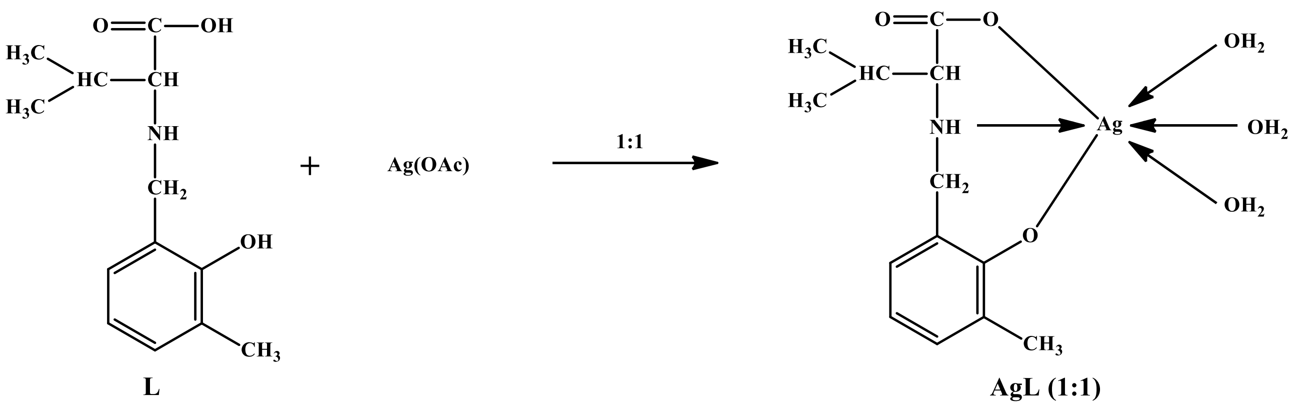

Scheme-II: Synthesis of silver complex

Journal of Chemical Health Risks
www.jchr.org
JCHR (2025) 15(6), 1189-1196 | ISSN:2251-6727

functional groups, with a broad band in the 3200–3500 cm^{-1} region due to O–H and N–H stretching and a sharp C=O stretching vibration of the carboxylic group around 1700 cm^{-1}. Upon coordination with Ag(I), distinct spectral changes are observed: the ν(C=O) band shifts to lower frequencies (~1610–1640 cm^{-1}), indicating deprotonation and binding through the carboxylate oxygen, while the broad O–H/N–H absorption band decreases in intensity and slightly shifts, suggesting involvement of hydroxyl/amine groups in complexation. Moreover, new absorption bands appear in the low-frequency region (500–700 cm^{-1}), which are attributed to Ag–O and Ag–N vibrations [9] (Fig. 1). These shifts and the emergence of metal–ligand bands confirm successful coordination of the ligand to Ag(I), as reflected in the comparative spectra (Table-1).

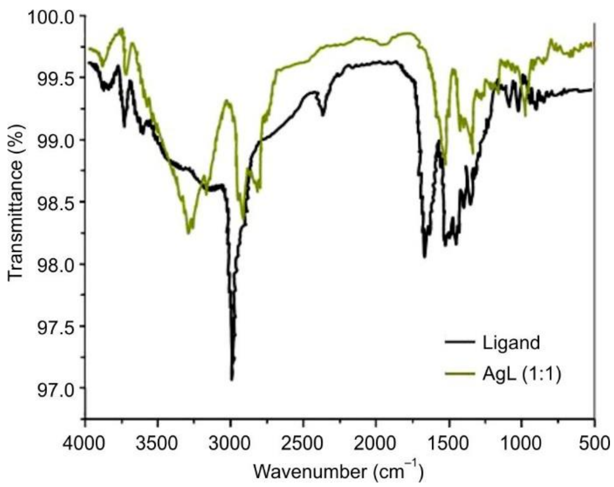

Fig 1. FT-IR spectra of ligand and its silver complex

3.1.2 NMR spectra: In ^{1}H NMR spectra, the free ligand shows the amide (–NH) proton at δ 8.83 ppm and phenolic –OH at δ 9.67 ppm, along with aromatic resonances between δ 7.18–6.99 ppm. Upon complexation with Ag, the –NH signal shifts downfield to δ 8.27 ppm [10,11], while the aromatic protons broaden slightly, indicating electronic perturbation from coordination. The aliphatic region (δ 3.9–1.0 ppm) shows moderate changes, consistent with altered electron density around the methylene and isopropyl groups (Fig. 2).

In the ^{13}C NMR spectra**,** the carbonyl (–COO) resonance shifts from δ 174.96 ppm in the free ligand to δ 168.28 ppm in the Ag(I) complex, confirming coordination *via* the carboxylate oxygen [12]. The phenolic carbon also shifts from δ 151.43 to δ 152.35 ppm, suggesting involvement of the –OH group in binding [13]. The methylene carbons adjacent to nitrogen and oxygen (δ 39.9–48.6 ppm) experience noticeable deshielding upon complexation, further supporting metal–donor interactions [14]. Overall, the systematic downfield and upfield shifts across both proton and carbon spectra validate that Ag coordinates through the –COO^{-}, –NH and phenolic –OH moieties, leading to redistribution of electron density and stabilization of the metal–ligand framework (Fig. 3).

3.1.3 UV spectra: The UV–Vis absorption spectrum of ligand L exhibits distinct bands at 294.69, 352.02 and 520.14 nm, attributable to π→π* and n→π* transitions, along with a weak charge-transfer feature. Upon coordination with Ag, these bands shift to ~301, ~360 and ~575 nm, indicating a bathochromic effect. The pronounced red-shift in the CT/MLCT region reflects ligand-to-metal charge transfer (LMCT) from oxygen and nitrogen donor atoms to the silver center, confirming effective chelation (Fig. 4). Furthermore, the visible-region tail of the AgL

TABLE-1
KEY FT-IR ASSIGNMENTS (cm^{-1}) OF LIGAND AND ITS SILVER COMPLEX

Frequency	Ligand	Metal Complex
ν (Phenolic –OH)	3200–3600 (broad, O–H stretching)	3300–3500 (O–H stretching, water)
ν (Aromatic C–H)	3000–3100 (C–H stretching)	3000–3100 (C–H stretching)
ν (Alkyl C–H)	2850–2960 (C–H stretching)	–
ν (Secondary Amine –NH)	3300–3500 (N–H stretching)	3200–3500 (N–H stretching, amide)
δ (Secondary Amine –NH)	1500–1600 (N–H bending)	–
ν (Carboxylic acid –COOH)	2500–3300 (O–H stretching)	–
ν (Carboxylic acid C=O)	1700–1750 (C=O stretching)	1600–1650 (asymmetric C=O stretching)
δ (Carboxylate –COO^{-})	–	1350–1450 (symmetric C=O stretching)
ν (Amide C=O)	–	1650–1690 (C=O stretching, amide)
ν (Aromatic C=C)	–	1450–1600 (C=C stretching, aromatic ring)
δ (Water H2O)	–	1600–1640 (H–O–H bending)
ν (Metal-Oxygen M–O)	–	400–600 (M–O stretching)
ν (Metal-Nitrogen M–N)	–	450–550 (M–N stretching)

Journal of Chemical Health Risks
www.jchr.org
JCHR (2025) 15(6), 1189-1196 | ISSN:2251-6727

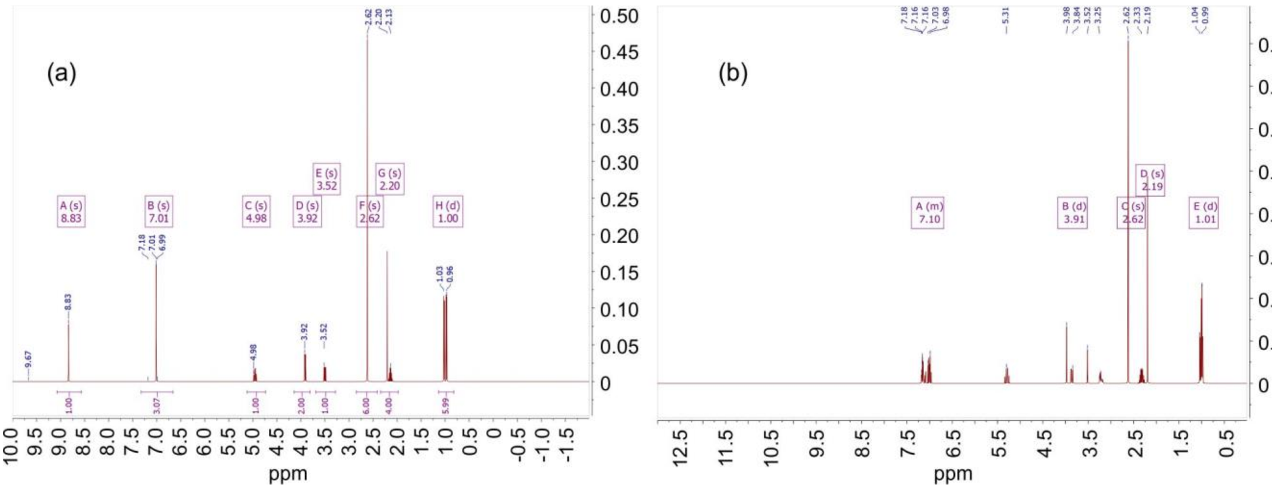

Fig. 2. [1]H NMR spectrum of ligand (a) and its silver complex (b)

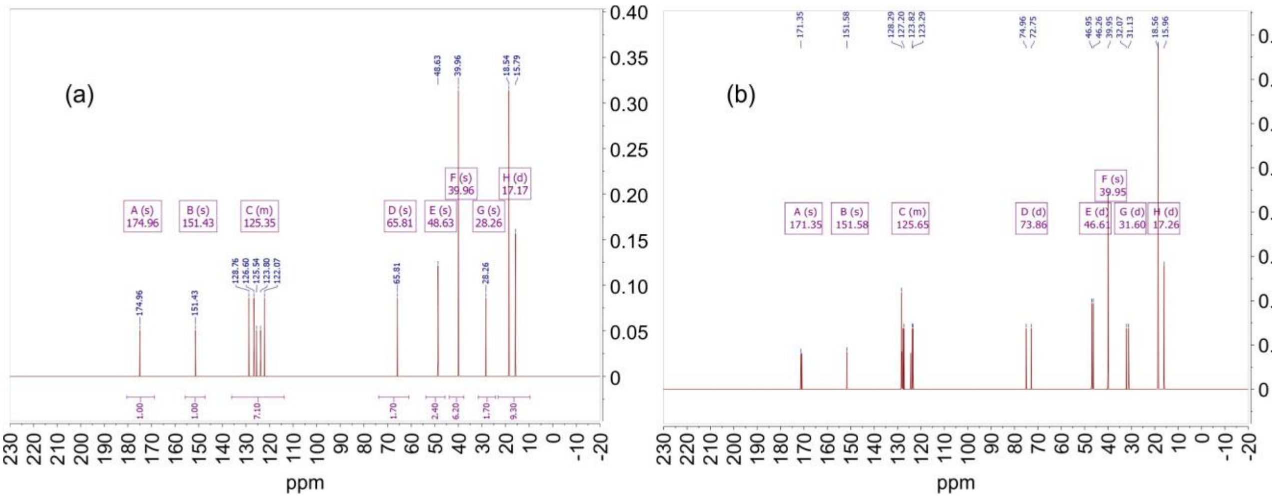

Fig. 3. [13]C NMR spectrum of ligand (a) and its silver complex (b)

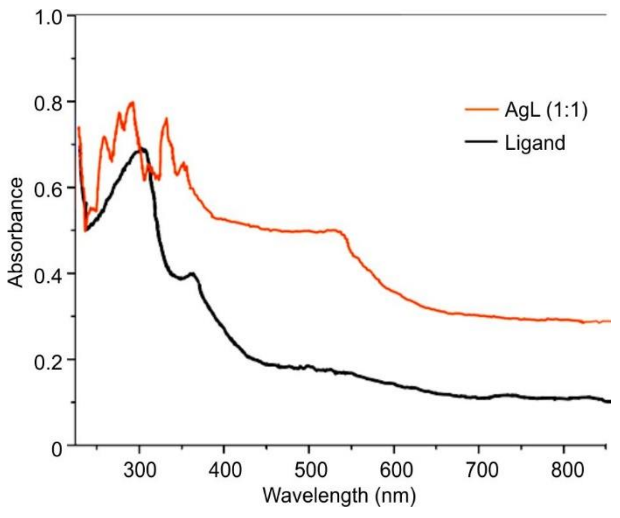

Fig. 4. UV spectra of ligand and its silver complex

complex becomes significantly more intense compared to the free ligand, suggesting enhanced π-conjugation and stabilization of the metal–ligand framework [15,16].

3.1.4 DFT: DFT optimization at the B3LYP/6-31G theoretical level reveals that the coordination of Ag with the ligand causes pronounced structural changes [17,18]. The formation of Ag–O (2.18–2.26 Å) and Ag–N (2.35 Å) bonds confirms successful metal–ligand interaction. Significant elongations such as C=O (1.24 → 1.30 Å) and C–N (1.47 → 1.52 Å) indicate electron redistribution upon chelation. The geometry around Ag deviates from ideal octahedral, with bond angles such as O18–Ag24–O22 (173.6º) and N23–Ag24–O19 (92.4º), reflecting a distorted coordination sphere (Table-2). These findings validate the participation of carbonyl and amine groups

Journal of Chemical Health Risks
www.jchr.org
JCHR (2025) 15(6), 1189-1196 | ISSN:2251-6727

TABLE-2
BOND LENGTH AND BOND ANGLES OF OPTIMIZED LIGAND AND ITS SILVER COMPLEX

L				AgL			
Bond	Bond length (Å)	Bond	Bond angle (º)	Bond	Bond length (Å)	Bond	Bond angle (º)
C16–N17	1.471	C16–N17–C18	119.915	C6–O19	1.43000	O18–Ag24–O20	87.694
N17–C18	1.457	C3–C4–O10	119.539	C10–N23	1.28752	O23–Ag24–O20	139.846
C18–C19	1.525	C19–O21–O20	62.681	C16–O18	1.39458	N23–Ag24–O22	141.837
C18–C26	1.568	C26–C28–C29	110.989	O18–Ag24	3.53864	O18–Ag24–O19	120.488
C26–C29	1.538	N17–C16–C3	118.713	Ag24–N23	3.54282	O24–Ag24–O22	78.317
C26–C28	1.541	C1–C2–C3	120.886				
C19–O20	1.245	C4–C4–C6	118.164				
C3–C16	1.526	C4–C4–C12	120.012				

in binding and highlight the predictive reliability of DFT in modeling Ag–ligand complexes (Fig. 5).

3.1.5 SEM: The SEM micrograph of the free ligand shows irregular, loosely packed nanosized particles with a rough and porous surface, indicating high surface area and partially amorphous morphology. After complexation with the metal, the SEM image reveals significant morphological changes, where the particles appear more compact, aggregated and denser with increased surface roughness (Fig. 6). These changes in particle size distribution and morphology confirm the successful coordination between the ligand and metal ions, leading to the formation of a stable metal complex with altered surface characteristics [19,20].

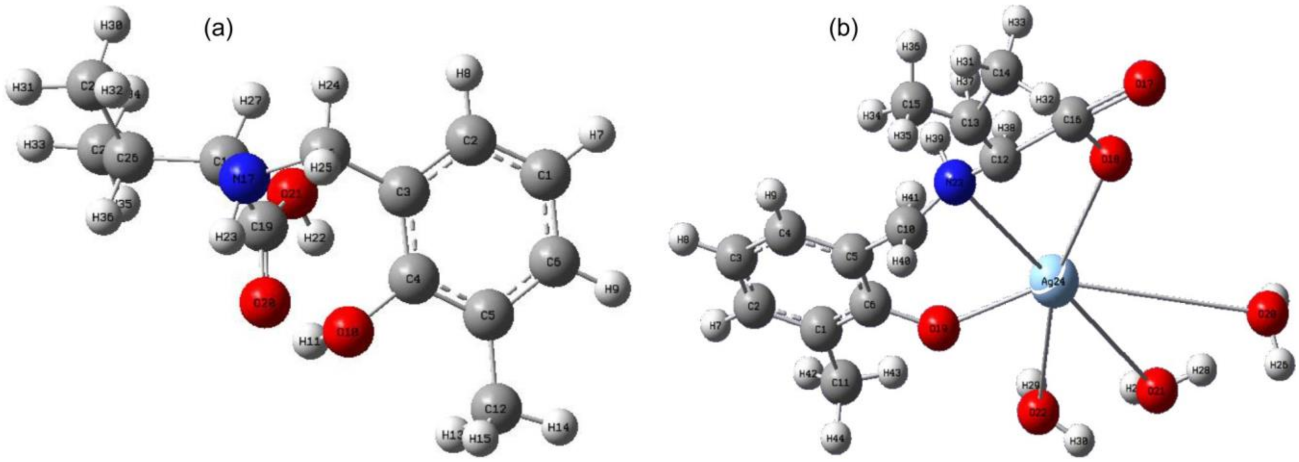

Fig. 5. Optimized structures of ligand (a) and its silver complex (b)

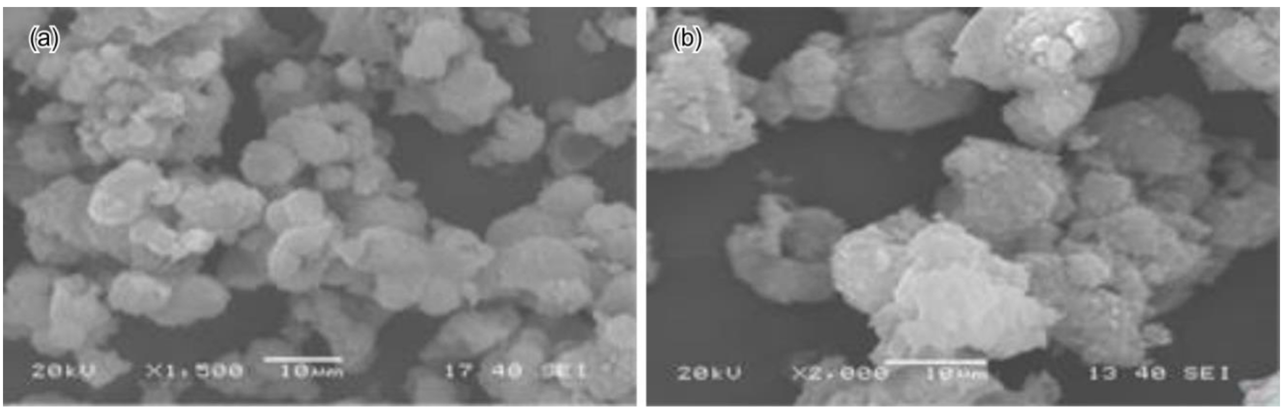

Fig. 6. SEM images of ligand (a) and its silver complex (b)

Journal of Chemical Health Risks
www.jchr.org
JCHR (2025) 15(6), 1189-1196 | ISSN:2251-6727

3.2 Anticancer activity: The comparative cytotoxicity evaluation revealed that silver complex (AgL) exhibited significantly higher anticancer activity compared to the free ligand. At lower concentrations, both compounds demonstrated moderate inhibition, but AgL consistently produced stronger cytotoxic effects across the tested range. At 1000 µM, free ligand retained 32.18% cell viability, whereas AgL reduced viability to 47.51%, indicating an enhanced anticancer potential (Fig. 7). The improvement can be attributed to the synergistic contribution of silver ions, which facilitate reactive oxygen species (ROS) generation and promote stronger interactions with cellular bio-molecules [21-23].

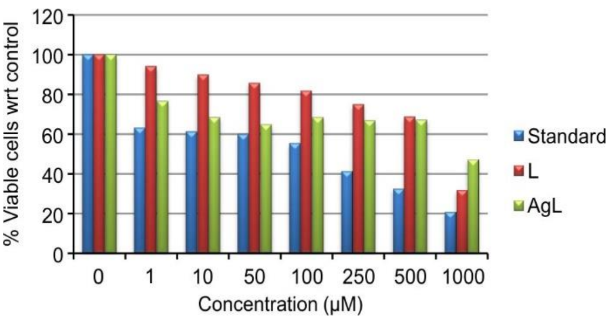

Fig. 7. Anticancer activity data of ligand and its silver complex

3.3 Antioxidant (DPPH) assay: The antioxidant assay further confirmed the superiority of silver complex over the free ligand. Free ligand demonstrated only modest free radical scavenging activity, reaching 29.75% inhibition at 1000 µM, whereas AgL exhibited a comparatively higher activity of 35.70% at the same concentration (Fig. 8). The enhanced performance of AgL suggests that silver coordination improves electron transfer efficiency, thereby increasing the radical quenching capacity of the ligand [24-26].

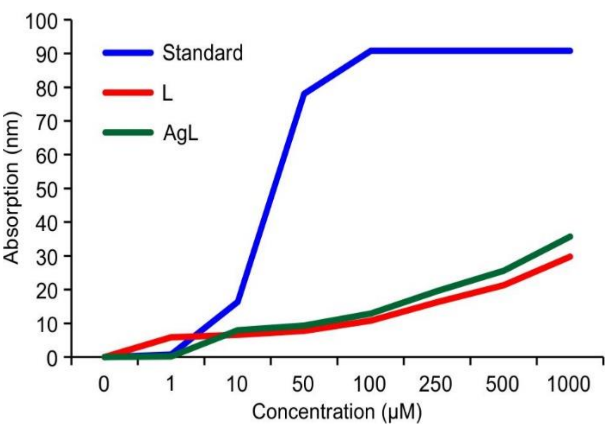

Fig. 8. Antioxdant response of ligand and its silver complex

3.4 Antimicrobial activity: The antimicrobial studies against *Escherichia coli* highlighted the greater efficacy of complex compared to free ligand. While both compounds showed dose-dependent inhibition, silver(I) complex consistently demonstrated better activity, particularly at lower concentrations. For instance, at 1 µg/mL, silver(I) complex achieved 52% inhibition compared to 48% for free ligand. Even at higher concentrations such as 1000 µg/mL, Ag(I) complex maintained 4% activity compared to 3% for free ligand, showing closer alignment with the standard ciprofloxacin (Fig. 9a). These results indicate that Ag(I) complex possesses enhanced antibacterial properties, likely due to the combined effect of silver's membrane-disrupting action and the ligand's intrinsic activity.

The antifungal assay against *A. niger* further emphasized the significant improvement of the silver complex over the free ligand. At 0.1 µg/mL, Ag(I) complex demonstrated 72% inhibition compared to only 45% for free ligand. At higher concentrations, free ligand activity diminished drastically, even recording negative inhibition values at 500 and 1000 µg/mL, suggesting a possible growth-promoting effect or resistance mechanism. In contrast, silver complex maintained basal antifungal activity (5% at 500 µg/mL and 2% at 1000 µg/mL), proving more stable and effective when benchmarked against amphotericin B [27,28] (Fig. 9b).

4. Conclusion

In this work, FTIR, NMR, UV and DFT studies confirmed the successful synthesis and structural integrity of the silver(I) complex. SEM analysis further supported complexation, showing a clear morphological transition from loosely packed, porous ligand particles to more compact and aggregated structures in silver(I) complex. The biological assays revealed that silver complex exhibited significantly enhanced anticancer, antioxidant and antimicrobial activities compared to the free ligand. The improvement can be attributed to the synergistic role of Ag(I) ions, which promote ROS-mediated cytotoxicity, increase radical scavenging efficiency and enhance microbial cell disruption. Overall, these findings demonstrate that silver coordination markedly augments the pharmacological efficacy of valine-derived ligands, establishing silver(I) complex as a strong candidate for future therapeutic applications.

Journal of Chemical Health Risks
www.jchr.org
JCHR (2025) 15(6), 1189-1196 | ISSN:2251-6727

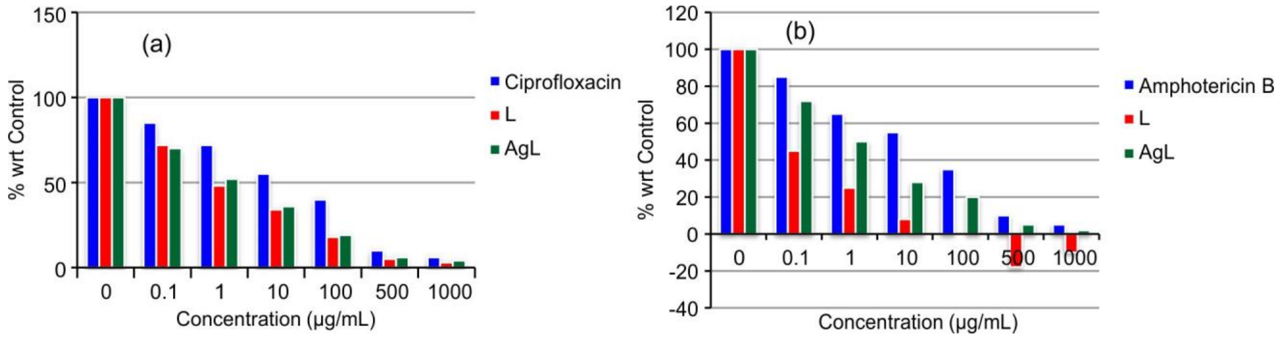

Fig. 9. (a) *E. coli* (antibacterial) and (b) *A. niger* (antifungal) activity data of ligand and its silver complex

References

1. Kim, S. Electrocatalytic and Enzymatic Inhibition by Metal Complexes. *Sci. Eng. Technol. Proc.* **3** (2025) 1–9. https://doi.org/10.71222/ah44z809
2. Rana, M. S., et al. A review on synthesis and biological activities of 2-aminophenol-based schiff bases and their transition metal complexes. *Appl. Organomet. Chem.* **38** (2024) e7724. https://doi.org/10.1002/aoc.7724
3. Kar, S. S., Misra, K. L., Swain, S. P. Recent Progress in Tailor-Tuned Metal–Amino Acid Frameworks: Broad Prospects in Pharmaceuticals. *ACS Appl. Mater. Interfaces* (2025). https://doi.org/10.1021/acsami.5c12805
4. Wang, T., Ménard-Moyon, C., Bianco, A. Self-assembly of amphiphilic amino acid derivatives for biomedical applications. *Chem. Soc. Rev.* **51** (2022) 3535–3560.
5. Wu, S., et al. Mechanisms Operating in the Use of Transition Metal Complexes to Combat Antimicrobial Resistance. *Microorganisms* **13** (2025) 1570. https://doi.org/10.3390/microorganisms13071570
6. Zia, A., et al. Pd-, Cu- and Ni-Catalyzed Reactions: A Comprehensive Review of the Efficient Approaches towards the Synthesis of Antibacterial Molecules. *Pharmaceuticals* **17** (2024) 1370.
7. Wang, X., Zhou, J., Wang, H. Bioreceptors as the key components for electrochemical biosensing in medicine. *Cell Rep. Phys. Sci.* **5** (2024) 101801. https://doi.org/10.1016/j.xcrp.2024.101801
8. Kuzderová, G., et al. Antimicrobial and anticancer application of silver (I) dipeptide complexes. *Molecules* **26** (2021) 6335. https://doi.org/10.3390/molecules26216335
9. Akash, M. S. H., Rehman, K. Comprehensive Insights into Infrared Spectroscopy. *Essentials of Pharmaceutical Analysis.* Springer Nature Singapore, Singapore, 2025, pp. 161–208. https://doi.org/10.1007/978-981-96-5996-8_4
10. Wu, M., et al. Discovery of Novel, Potent, Orally Bioavailable and Efficacious, Hypoxia-Inducible Factor Prolyl Hydroxylase Inhibitors for Hematopoietic Stem Cell Mobilization. *J. Med. Chem.* **68** (2025) 6386–6406. https://doi.org/10.1021/acs.jmedchem.4c02889
11. Gündüz, M. G., et al. Biginelli dihydropyrimidines and their acetylated derivatives as L-/T-type calcium channel blockers: Synthesis, enantioseparation and molecular modeling studies. *Arch. Pharm.* **358** (2025) e2400584. https://doi.org/10.1002/ardp.202400584
12. Refat, M. S., et al. Synthesis and characterization of complexes formed by Fe(III), Cr(III), Co(II), Cu(II), Cd(II) and Ag(I) ions with the drug captopril and the amino acid glycine. *Bull. Chem. Soc. Ethiop.* **39** (2025) 1137–1152. https://dx.doi.org/10.4314/bcse.v39i6.9
13. Xiang, Y., et al. Insights into structure-antioxidant activity relationships of polyphenol-phospholipid complexes: The effect of hydrogen bonds formed by phenolic hydroxyl groups. *Food Chem.* (2025) 144471. https://doi.org/10.1016/j.foodchem.2025.144471
14. Akash, M. S. H., Rehman, K. Comprehensive Insights into Nuclear Magnetic Resonance Spectroscopy. *Essentials of Pharmaceutical Analysis.* Springer Nature Singapore, Singapore, 2025, pp. 439–532. https://doi.org/10.1007/978-981-96-5996-8_10

15. Mandal, S., Das, G., Askari, H. *RSC Adv.* **4** (2014) 24796. https://doi.org/10.1039/C4RA01288G
16. Musa, S., Idris, S. O., Onu, D. A., Suleiman, A. B. *Avicenna J. Environ. Health Eng.* **6** (2019) 100. https://doi.org/10.34172/ajehe.2019.13
17. Łaski, P., et al. Capturing the short-lived excited singlet state in a TADF silver(I) complex crystal. *Chem. Commun.* (2025). https://doi.org/10.1039/D5CC04193G
18. Ebied, M. S., Elnobi, S., Abuelwafa, A. A. Structural and optical properties of spin coated ZnTTBPc thin films for optoelectronics via DFT and experiments. *Sci. Rep.* **15** (2025) 36301. https://doi.org/10.1038/s41598-025-21726-
19. 19.1 Nithiasri, P. R., Aarthi, J., Karthikeyan, B. Novel self-assembled valine-derived carbon-supported Ag@ZnO optical materials for enhanced photodegradation and anti-bacterial activity. *Nanoscale Adv.* **7** (2025) 5323–5336. https://doi.org/10.1039/D5NA00427F
20. Saranya Parvathi, S., et al. Amino acid cross-linked PVA–silver composites: preparation and analysis of material and catalytic properties. *Chem. Pap.* (2025) 1–14. https://doi.org/10.1007/s11696-025-04265-4
21. Aboul-Nasr, M. B., et al. Exploring the anticancer potential of green silver nanoparticles–Paclitaxel nanocarrier on MCF-7 breast cancer cells: an in vitro approach. *Sci. Rep.* **15** (2025) 20198. https://doi.org/10.1038/s41598-025-06275-4
22. Raju, S. K., et al. Silver complexes as anticancer agents: A perspective review. *Ger. J. Pharm. Biomater.* **1** (2022) 6–28. https://doi.org/10.5530/gjpb.2022.1.3
23. Danışman-Kalındemirtaş, F., et al. Selective cytotoxicity of paclitaxel bonded silver nanoparticle on different cancer cells. *J. Drug Deliv. Sci. Technol.* **61** (2021) 102265. https://doi.org/10.1016/j.jddst.2020.102265
24. Adeleke, A. A., et al. Evaluation of substituent bioactivity and anion impact of linear and T-shaped silver(I) pyridinyl complexes as potential antiproliferative, antioxidant, antimicrobial agents and DNA- and BSA-binders. *New J. Chem.* **45** (2021) 17827–17846. https://doi.org/10.1039/D1NJ03231C
25. Rana, M. S., et al. Antioxidant activity of Schiff base ligands using the DPPH scavenging assay: an updated review. *RSC Adv.* **14** (2024) 33094–33123. https://doi.org/10.1039/D4RA04375H
26. Gorkanti, S., Dasari, A., Padma, S. M. Design, synthesis, characterization, catalytic, fluorometric sensing, antimicrobial and antioxidant activities of Schiff base ligand capped AgNPs. *J. Fluoresc.* **32** (2022) 2363–2378. https://doi.org/10.1007/s10895-022-03026-w
27. Khan, M., et al. Potent in vitro antibacterial and antifungal activity of novel ciprofloxacin–silver complex. *J. Chem. Res.* **49** (2025) 17475198241311777. https://doi.org/10.1177/17475198241311777
28. Lima, B. G. A., et al. Synthesis and characterization of silver nanoparticles stabilized with biosurfactant and application as an antimicrobial agent. *Microorganisms* **12** (2024) 1849. https://doi.org/10.3390/microorganisms12091849